Large wildfires in western US exacerbated by tropospheric drying linked to a multi-decadal trend in the expansion of the Hadley Circulation

Authors: L. Zhang[1], W. Lau[2]*, W. Tao[2,3], Z. Li[1,2]

[1]Department of Atmospheric and Oceanic Science, University of Maryland, College Park, MD, USA

[2]Earth System Science Interdisciplinary Center, University of Maryland, College Park, MD, USA

[3]State Key Laboratory of Numerical Modeling for Atmospheric Sciences and Geophysical Fluid Dynamics, Institute of Atmospheric Physics, Chinese Academy of Sciences, Beijing, China

Submitted to *Geophys. Res. Lett.*

April 2020

*Corresponding author: William K. M. Lau Email: wkmlau@umd.edu

Abstract: Analyses of wildfire-climate relationships over North America were conducted using diverse data including ground-based measurements, satellite retrievals, and re-analyses for the period 1984-2014. Results show the western US (WUS) has experienced the most robust trend in increasing burned area, even though Alaska and central Canada possess comparable or even stronger warming trends compared to WUS. In addition to warming, the WUS has been under the influence of multi-decadal trends in tropospheric relative humidity deficit, reduced cloudiness, increased surface net insolation, enhanced adiabatic warming and drying from increased tropospheric subsidence, as well as drying from enhanced off-shore low-level flow, potentially leading to more abundant dry fuels and raging large wildfires. These trends are likely the manifestation of a regional climate feedback that is enabled by the intensification, and expansion of the North Pacific Subtropical High, associated with a widening of the subsiding branch of the Hadley circulation under greenhouse warming.

Plain language summary: Our observational analyses show that increasing wildfires in the western US are linked to a multi-decadal drying trend of the subtropical troposphere, associated with the expansion of the Hadley circulation under greenhouse warming. The circulation change induces a regional climate feedback, involving reduced relative humidity, less cloud, more downward surface insolation, warmer land surface, enhanced subsidence and stronger off-shore low-level winds resulting in accelerated, and sustained tropospheric warming and drying that exacerbate wildfires over the WUS. Results suggest that the WUS wildfire situation is expected to worsen quickly, if actions to combat climate change are not taken soon.

Keywords: Wildfire； Relative humidity； Hadley circulation； Global warming

1 Introduction

Staggering socio-economic losses stemming from more frequent and severe wildfires over North America in recent decades have drawn much attention to the need for better understanding of causes of increased wildfires, in order to inform and provide sound strategies for mitigation. Numerous previous studies have found significant increasing trends in occurrence, total burned area, and duration of wildfires over western US, most pronounced in the forests of Northern US Rocky Mountains (Dennison et al., 2014; Westerling et al., 2006). Burned area of large fires have doubled over boreal region of Canada and Alaska from 1959-1999 (Kasischke et al., 2006). These increased wildfire activities have been linked to natural climate variability and to human activities (Abatzoglou and Williams, 2016; Balch et al., 2017; Harvey, 2016; Littell et al., 2009). Warmer temperature, earlier snowing melting, prolonged summer drought, vegetation types and increased lightning are believed to be key factors contributing to the frequency, severity, and length of wildfires (Holden et al., 2018; Littell et al., 2016; Running, 2006; Veblen et al., 2000; Veraverbeke et al., 2017a; Westerling et al., 2003, 2006). The aforementioned studies and others have led to a conclusion in the Fourth National Climate Assessment Report, U.S. Global Change Research Program (Wuebbles, 2017): *The incidence of large forest fires in western United States and Alaska has increased since the early 1980 (high confidence) and is projected to further increase in these regions as the climate warms with profound change to certain ecosystems (medium confidence).*

Contemporaneously, there have also been multiple evidences indicating that prolonged drought, associated with expansion of the semi-arid and desert regions in the globe in recent decades are likely associated with greenhouse warming, and that global drying are projected to get worst in the future (Dai, 2006, 2011; Feng and Fu, 2013; Huang et al., 2016; Lau and Kim, 2015; Seager and Vecchi, 2010; Zeng and Yoon, 2009). Modeling studies have suggested that increased

atmospheric dryness, *i.e.*, reduction in relative humidity (RH) and increased frequency and duration of dry spells in subtropics and midlatitudes located over western regions of major continents may be a component of a canonical global pattern of precipitation and large-scale circulation in response to greenhouse warming (Lau et al., 2013). This pattern involves changes in the Hadley circulation (HC), linking a narrowing of the ITCZ with enhanced precipitation, to an expanding subtropical subsiding zone with reduced relative humidity (RH) in the mid and lower troposphere, via the so-called Deep Tropical Squeeze (DTS) radiation-dynamical feedback effects (Lau and Kim, 2015). Reduction in RH is important to the occurrence and spread of wildfires because of its close relationship to the water stress on vegetation. Low surface RH and high temperature increase the vapor pressure deficit (VPD), enhance evaporative demand, and accelerate drying of vegetation, resulting in increased fire fuels and potential for large and severe wildfires (Seager et al., 2015, Holden et al., 2018; Williams et al., 2014). Up to now, the physical relationships among wildfires in North America, regional feedback processes, and changes in the large-scale circulation, global dryness, and linkages to greenhouse warming are still poorly understood. In this paper, we aim to provide observational evidences revealing these relationships and shed new lights on underlying regional feedback processes affecting wildfires trends in North America. We use multiple sources of data for burned area and key climate control variables, *i.e.*, surface air temperature, surface relative humidity, cloudiness, net surface incoming solar radiation, and Palmer's drought precipitation index (PDSI) over North America from in situ and satellite observations, as well as tropospheric temperature, relative humidity, winds, and sea level pressure from five re-analyses products for the period 1984-2014.

2 Methods

Data analyses were conducted using multiple independent datasets of wildfires and climate control variables. For wildfire data, we used the burned area information available from the MTBS database (Eidenshink et al., 2007) and Canada NFDB database. MTBS maps the burned area across all lands in the U.S from 1984 to present, including all fires 1000 acres or greater in the western US and 500 acres or greater in the eastern US. Burned area were mapped by using Landsat reflectance data to generate a Normalized Burn Ratio (NBR) for each pre-fire and post-fire target areas and then create a differenced Normalized Burn Ratio (dNBR). In our study, a total of 12,279 large wildfires were examined for U.S from MTBS dataset. Although large wildfires account for small portion of total number of wildfire frequency, these large wildfires contribute to nearly 95% of total burned area. In addition, we used the Canadian National Fire Database (CNFDB) for the region of Canada. This collection of forest fire data is available from the Canadian fire management agencies. Unlike MTBS, NFDB dataset includes all sizes of forest fires. We selected the wildfires with size larger than 500 acres to be consistent with MTBS. For NFDB, a total number of 13,614 large fire were examined.

For climate control variables, we used relative humidity (RH) from HadISDH global monthly land surface dataset (latest version 4.0.0.2017f) provided by the Meteorological Office Hadley Centre, which is derived from quality controlled sub-daily HadISDH stations since 1973. The RH data are monthly gridded at 5° by 5° resolution. Despite its relative coarse spatial resolution, it is a unique, in situ observations-only climate-data gridded product that is homogenized and physically consistent (Smith et al., 2011; Willett et al., 2014). Total cloud amount was obtained from the International Satellite Cloud Climatology Project (ISCCP). The new H-series of ISCCP extends the period of record to 1982-2014, providing monthly averages of cloud properties at 1° spatial resolutions (Rossow and Schiffer, 1991). Shortwave radiative fluxes data is available from

Surface Radiation Budget (SRB) from NASA, which covers a 24 year (1984-2007) with 1º x 1º global grid derived from satellite-derived cloud parameters, reanalysis meteorology, plus a few other ancillary data sets. For drought estimates, we used the Palmer Drought Severity Index (PDSI) from NCAR (Dai et al., 2004), which uses both temperature and precipitation data to estimate relative dryness PDSI. The monthly gridded air temperature (land) used are from University of Delaware, this product uses a large number of station data, including the GHCN2 (Global Historical Climate Network), and complements the ICOADS (International Comprehensive Ocean-Atmosphere Data Set) dataset. For large scale circulation analysis, we used five reanalysis products from MERRA2, NCEP2, ERA-Interim, JRA55, and 20CR respectively (Compo et al., 2011; Dee et al., 2011; Gelaro et al., 2017; Kanamitsu et al., 2002; Kobayashi et al., 2015) (See Table S2, for more detailed information for each dataset).

In our analysis, we focused on burned area data for the fire season, i.e., May to September, selecting only those identified as wildfires (natural). All fires labeled as prescribed (man-make) fires were excluded. To facilitate quantitative analysis, we processed the above burned area data into 1° x 1° spatial grid data on monthly temporal resolution. Similarly, the original NFDB data were processed to 1° x 1° grid data as MTBS. Reanalysis datasets for meteorology were remapped onto a uniform 2.5°×2.5° grid by using bilinear interpolation to calculate the multi-reanalysis ensemble mean.

Our analyses consist of three parts. First, analysis was conducted for wildfire datasets for the entire North America, to identify regions with pronounced regional trends in wildfires and surface air temperature. Second, trend patterns of key climate control variables of surface relative humidity, cloudiness, net downward surface solar radiation, and drought severity were constructed and examined for correlations with wildfire trends for each sub-region of WUS, AK and WCC

respectively. Third, circulation and precipitation features associated with global warming trends over the North Pacific and North America, as well as vertical profiles of temperature, RH and vertical motions are examined over each subregions of WUS, AK and WCC using ensemble mean of five re-analysis products. Trends for all variables including fire records and climate variables are based on linear regression as default. The correlation between burned area and various climate variables used Pearson correlation. Student-*t* test was used to assess the significance (p-values) of monotonic trends in fire and climate variables.

3 Results

3.1 Wildfires trends over North America

To begin, we examine the time variations and trends of large fire burned area, and surface air temperature averaged over North American (NA), and separately for US and Canada. The NA time series of burned area (Fig.1a) shows large interannual variability, and a strong positive trend during 1984-2014. The positive trend of burned area over NA is statistically significant ($p < 0.05$), as found in previous studies (Dennison et al., 2014; Picotte et al., 2016). The average of total burned area in the 2010's is more than double the mean during the1980's. Separating into US and Canada regions, it can be seen that the increasing wildfires trend is mainly contributed by US, while Canada shows considerable variability but no significant long-term trend. On the other hand, area-averaged surface temperature (Fig.1b) shows similar warming trend (+0.3 ^{o}C decade^{-1}) and variability for both US and Canada. In contrast to the trends in wildfire burned area, the NA warming appears to be driven more by the warming of Canada than the US. Hence, on a continental scale, a warmer temperature appears to be a necessary but not sufficient condition for increased wildfires over North America. To understand the differences between the warming and wildfire

trends in US and Canada, we need to examine their spatial distribution, and relationships with the regional and global climate forcing and feedback.

The spatial pattern of large fire burned area trend over NA during 1984-2014 (Fig.1c) is highly asymmetric in the sense that while both negative and positive trends are present, significant signals ($p<0.05$) are found clustered only in regions with positive trends. No significant clusters of negative trends are found. Three regions of strongly increasing trend in burned area (> 50-100 km^2 $decade^{-1}$) stand out: western US (WUS), Alaska (AK), and Western-Central Canada (WCC). WUS includes states of Washington, Oregon, northern California, Idaho, and mountain regions of Arizona and New Mexico. WCC includes provinces of Alberta, Saskatchewan and southern Northwest Territories. Negative but weaker trends ($p>0.05$) in burned area are found over the center and west of Northwest Territories, Manitoba and part of Quebec province. Over WUS, the burned area shows a robust, steady long-term trend (total area of 3350 km^2 $decade^{-1}$) with strong interannual variability (Fig.1d). In contrast, for AK and WCC, trend signals are much weaker, and appear to be affected by episodic occurrences of a few exceptionally large fires (Fig.1e, f). The asymmetry and highly regional distributed trend pattern in burned area, as well as different temporal variability among WUS, AK and WCC suggest the effect of a large-scale background forcing, *i.e.*, overall warming of North America (Fig.S1), modulated by regional scale climate feedback processes.

3.2 Related trends in key climate control variables

As discussed previously, a reduction in RH will likely lead to increased surface VPD resulting in accelerated drying of the vegetation, and increased potential for wildfires (Holden et al., 2018; Williams et al., 2014). Furthermore, a long-term in tropospheric RH deficit is also likely associated with suppressed clouds and precipitation. Less clouds will lead to reduced SW cloud

shielding, enhanced incoming surface SW radiation, resulting in sustained warming and drying of the atmosphere-vegetation system, with enhanced wildfires. For convenience, we refer to this chain of processes as the regional climate feedback enhancing wildfires (RCFW). In the following, we examine the validity of RCFW in affecting the long-term trends in wildfires over NA, by conducting trend and correlation analyses on wildfires burned area with respect to several key climate control variables, *i.e*., surface RH, cloud amount, shortwave downward radiation (SWDR) and PDSI. The trend patterns of these climate observables for the wildfire season (May-September) are shown in Fig.2. Overall, a north-south dipole pattern in reduced surface RH is found over North America, with strong negative trends (2-3% decade^{-1}) over the southern and western US, and positive trends over northern Midwest and central Canada (Fig.2a). Over Alaska, the RH trend signal is mixed. Total cloud cover (Fig.2b) shows reduction in broad swath spanning Alaska, Northwest territories the US Midwest and Eastern US, with the maximum reduction (10-15% decade^{-1}) over the WUS. The overall reduction in cloudiness is comparable to previous studies which showed overall reduction in cloudiness up to 5% decade^{-1} for contiguous US over a similar period (Free et al., 2016; Sun et al., 2015). Increased SWDR is found over the WUS, coinciding with the regions of strong reduction of clouds and reduced surface RH (Fig.2c). Over northwestern Canada, SWDR trends negative, except in southern Alaska, just north the Gulf of Alaska, where the trend is weakly positive. The strong positive SWDR trend over WUS is consistent with the 'global brightening' since mid-1980 (Wild, 2011), attributable in part to reduced cloudiness and aerosols. From PDSI (Fig.2d), it can be seen that a large part of the southern and WUS, central Canada and part of southern Alaska are experiencing increasing drought conditions (negative PDSI).

Based on the above results, we select for further analyses the areal mean serial correlations of burned areas to RH, cloud amount, SWDR and PDSI respectively for three key regions of WUS, AK and WCC that show strong positive trends in large wildfires burned areas (See Fig. 1c). During the last three decades, WUS has experienced decreasing RH (~ 0.7% decade^{-1}, Fig.2e), decreasing cloud amount (5.9% decade^{-1}, Fig.2f), increasing SWDR (~5.7 W/m^2 decade^{-1}) reached the land surface (Fig.2g), and increasing drought severity (negative trend of 0.4 % decade^{-1} in PDSI, Fig.2h). Worth noting is that all the aforementioned climate observables show considerable interannual-to-interdecadal variability, linked to natural modes of climate variability such as ENSO, PDO and AMO, that could influence the conditions of fire weather, fuel, ignition by lightning, frequency, duration and intensity of wildfires (Kitzberger et al., 2007; Pan et al.,2018; Schoennagel et al., 2005; Wang et al., 2014). Taken into account both trends and natural variability, the strongest correlations with burned area are in descending order reduced RH (-0.65, $p<0.01$), cloud amount (-0.56, $p<0.01$), SWDR (+0.49, $p<0.05$) and PDSI (-0.45, $p<0.05$) supporting RCFW (Fig.2 i-l).

Correlation analyses were carried out for AK and WCC similar to WUS, and results for all three regions are summarized in Table S1. Robust trends of burned area and significant correlations with all four climate observables are found only in WUS. For AK, no significant correlations are found in any of the climate observables. For WCC, significant relationships ($p<0.05$) are found only in RH and PDSI. These suggest that RCFW works for WUS only, but not for AK and WCC. The reasons for the regional differences are explored in the next section.

3.3 Wildfires and Greenhouse Warming

Previous observational and modeling studies have identified features in the large-scale circulation that are likely attributable to greenhouse warming. These include among others, multi-

decadal trends in a strong warming and moistening of the tropical atmosphere (Fu et al., 2011; Lau et al., 2013; Santer et al., 2008, 2016); a rise of the tropical tropopause (Lorenz and DeWeaver, 2007; Seidel and Randel, 2007); a widening of the subtropics and poleward migration of midlatitude storm tracks (Feng & Fu, 2013; Hu & Fu, 2007; Lu et al., 2007; Seidel et al., 2008; Yin, 2005), and expansion of the global dry lands including the WUS (Seager and Vecchi 2010, Dai, 2011; Huang et al., 2016). More recently, CMIP5 model results have demonstrated that the aforementioned changes are underpinned by the "Deep Tropical Squeeze" (DTS) *i.e.*, a structural change in the Hadley Circulation (HC) under greenhouse warming, featuring a narrowing ITCZ core with increased precipitation, linked to increased subsidence and reduced RH in a widening subtropics and poleward shift of the storm tracks (Fu, 2015; Lau and Kim, 2015).

In the following, we examine the changes in the large-scale circulation affecting the northeastern Pacific and North America climate using re-analyses data, in order to shed new light on the possible relationship between wildfires in North America and greenhouse warming. To increase the robustness of the results, we have computed the long-term trend patterns of tropospheric temperature, RH, sea level pressure, winds, vertical motion, and precipitation for 1984-2014, based on the ensemble mean of 5 independent re-analyses datasets i.e., MERRA2, ERA-Interim, NCEP2, JRA55 and 20CR (see Table S2 for detailed description of each dataset)

As revealed in the latitude-height cross-section of zonal annual mean temperature trend pattern (Fig.3a), during 1984-2014, there has been strong warming of the entire troposphere and cooling in the lower stratosphere (above 150 hPa) - a well-recognized signature of global greenhouse warming (Fu et al., 2011; Santer et al., 2008, 2016). Associated with the tropospheric warming, the RH trend (Fig.3b) displays a characteristic pattern indicating increased RH in the deep tropics, but strong RH reduction in the tropical upper troposphere, and descending arms of

regions of RH deficit in the tropospheric column to the earth surface in the subtropics and midlatitudes of both hemispheres. The RH trend pattern is similar to model projections attributable to global warming (Sherwood et al., 2010). The pattern can be understood in terms of the faster rate of increased saturated vapor pressure with temperature as governed by the Clausius-Clapeyron law of thermodynamics, compared to the actual increase in ambient vapor pressure due to transport processes (Lau and Kim, 2015). Increased dry advection from above by enhanced anomalous descent in the subtropics and mid-latitudes due to the expansion of the HC under greenhouse warming can lead to further RH deficit in the lower troposphere and near surface over these regions (Hu and Fu, 2007; Lau and Kim, 2015). In association with the trend in reduced zonal mean RH, an east-west dipole anomalous sea-level pressure (SLP) pattern, with high SLP centers over the North and East Pacific and WUS coupled to low SLP centers over the rest of North America is established during the peak wildfires season (May-September), signaling an intensification and expansion of the North Pacific Subtropical High (NPSH, Fig.3c). The eastward extension of the NPSH, signaled by the development of an anomalous high SLP center over WUS, is likely to be strongly affected by regional topographic effects. Specifically, an anomalous anticyclonic circulation center is found anchored over the elevated arid region of the Great Basin east of the Rocky Mountains (Fig.3c). As the cold, dry air masses descend in a clockwise rotation from high-elevations into lower valley regions of the coastal mountain ranges they are heated by adiabatic compression, causing a further rapid drop in relative humidity, and gusty winds due to air density differences. These hot and dry off-shore winds combined with dry vegetation during summer and fall, would fan more severe wildfires, and likely spur a prolonged fire season (Guzman-Morales and Gershunov, 2019; Hughes et al., 2011; Jin et al., 2015; Miller and Schlegel, 2006; Yue et al., 2014).

Strong trends in suppressed precipitation, and widespread anomalous sinking motion at 500 hPa are found over much of the subtropical and mid-latitude regions of Northeast Pacific and North America (Fig.3d). Also found are strong reduction in precipitation in the northern edge of the ITCZ near 10-15^{o}N, and increased precipitation near the equator. These features mirror those associated with the DTS, under global warming (Lau and Kim, 2015). Note that the WUS is geographically located at the semi-arid zone at the eastern edge of the North Pacific Subtropical High. Hence it is possible that changes in the RH, cloudiness, SWDR, precipitation, and circulation arising from tropical influence due to global warming may affect wildfires in WUS region more strongly compared to other regions in North America. This may explain, in part, the lack of strong and coherent signals related to burned areas in our chosen climate control variables, in the other two regions with significant burned area trends, *i.e*., AK and WCC. In these two regions, influence from other factors such as storm track and jet stream dynamics, as well as increased lightning ignitions and northward expansion of the boreal forest associated with Arctic warming may play more important roles (Box et al., 2019; Veraverbeke et al., 2017).

To further explore RCFW over WUS, we examine the trend patterns in vertical profiles of RH, vertical p-velocity (omega) and temperature from the multi-reanalysis data averaged over WUS (Fig.3e) during the wildfire season (May-September). Most noteworthy is the robust warming trend (0.3-0.5 C decade^{-1}) of the atmospheric column from surface to above 200 hPa. A strong trend in sinking motion (positive omega) is found from 800hPa to 150hPa with a maximum rate of up to 1.5 10^{-3} Pa/s decade^{-1} near 400 hPa. As discussed previously, both increased temperature and subsidence can lead to large RH deficit. The RH profile shows reduction over the entire atmospheric column, with maxima decreasing trend about 2% decade^{-1} at the 300hPa, and a secondary maximum (1% decade^{-1}) near 850 -900 hPa. This secondary low-level maximum RH

reduction is likely related to the dry advection effect of the enhanced offshore low-level flow, as well as increased intensity of warmer and drier winds by adiabatic compression, descending from higher elevation inland to coastal areas across the central and southern WUS region (See discussion for Fig.3c). As shown previously (see Fig.2), the RH deficit is associated with reduced cloud and precipitation and increased surface solar radiation that is likely to enhance the warming of the earth surface. Additionally, adiabatic warming of the descending air would enhance the warming of the atmospheric column, further reducing RH. These feedback processes would thus amplify the greenhouse warming and drying of WUS atmosphere-land system. At the same time, reduced RH leads to increased VPD, enhanced evapotranspiration from leaves and thus accelerates the drying of the vegetation and land, promoting more wildfires. Over AK and WCC (Fig.3f, g), while the tropospheric warming signal is strong, RH and vertical motion do not show coherent signals in the vertical, indicating a lack of RCFW.

4 Conclusion and Discussion

Our analyses of long-term wildfire trends over North America revealed that the most significant increasing trend of large wildfires over North America is in the Western US, even though temperature rise is more pronounced at high latitudes over Alaska and Canada. A plausible explanation is put forth, involving regional climate feedback enhancing wildfire (RCFW) as follows. A RH deficit associated with drying of the subtropics under global warming inhibits convection, suppresses cloudiness and precipitation, and minimizes the shortwave cloud shielding effect, resulting in enhanced net downward surface shortwave radiation. The increased shortwave radiation accentuates an already warming land-atmosphere system, and through RCFW amplifies the RH deficit, increasing the VPD and drying of vegetation, and potentially spurring more severe

wildfires. The RCFW response over western US is likely a regional manifestation of a global drying trends associated with the expansion of the subsidence branch of the Hadley Circulation (HC), coupled to increased precipitation of the ITCZ in the deep tropics, that have been attributed to greenhouse warming in previous studies (Hu and Fu, 2007; Lau and Kim, 2015). Our results also show that the development of an anomalous high surface pressure center over the Great Basin in associated with global drying trend and HC changes, may be instrumental in enhancing offshore winds, fanning more large wildfires over the WUS.

The Western US, being geographically located over the subtropical semi-arid zone at the eastern edge of the North Pacific Subtropical High, is more likely subjected to the strong influence from the Hadley Circulation expansion and RCFW. Over Alaska, and Western Central Canada, the other two regions in North America with significant, but weaker long-term trends in large wildfire burned area, RCFW is found to be weak or absent. We suggest this may be due to the high-latitude locations of these regions, where tropical influences, such as DTS, on wildfires are diminished. The wildfires burned area in these regions may be more impacted by additional climate controls such as storm track and jet stream dynamics, as well as possibly increased lightning ignition, and northward migration of the boreal forest associated with Arctic warming (Box et al., 2019; Veraverbeke et al., 2017b). Finally, it remains to be investigated if RCFW is operative over other continental vegetated land regions (Asia, Europe, South Africa, Australia, and South America) affected by global warming and atmospheric drying. If so, more wildfires on a global scale is likely to increase emissions of greenhouse gases, and light-absorbing aerosols such as black carbon and organic carbon which can further warm the atmosphere-land surface by absorption of solar radiation, and reduction of snow albedo, exacerbating greenhouse warming,

thus completing the climate-wildfire feedback loop (Liu et al., 2010, 2014). These are important subjects for future studies.

Acknowledgments

This work is supported by the NASA National Climate Assessment Program (NNH14ZDA001N-INC). All data used in this work are available online: Burned area data is used from MTBS (www.mtbs.gov) and Canada National Fire Database (https://cwfis.cfs.nrcan.gc.ca/datamart); surface RH observation (www.metoffice.gov.uk/hadobs/hadisdh/); ISCCP cloud data (https://isccp.giss.nasa.gov/); surface radiation product from_NASA/GEWEX Surface Radiation and Budget data sets (https://eosweb.larc.nasa.gov/project/srb); PDSI data from NCAR (https://climatedataguide.ucar.edu/climate-data/palmer-drought-severity-index-pdsi); Five reanalysis datasets used including MERRA2 (https://gmao.gsfc.nasa.gov/reanalysis/MERRA-2/); JRA55(https://climatedataguide.ucar.edu/climate-data/jra-55); 20th Century Reanalysis (https://www.psl.noaa.gov/data/20thC_Rean/); NCEP/DOE Reanalysis 2 (R2) Project datasets (https://climatedataguide.ucar.edu/climate-data/ncep-reanalysis-r2) and ERA-Interim data (https://www.ecmwf.int/en/forecasts/datasets/reanalysis).

References

Abatzoglou, J. T., & Williams, A. P. (2016). Impact of anthropogenic climate change on wildfire across western US forests. *Proceedings of the National Academy of Sciences*, *113*(42), 11770–11775. https://doi.org/10.1073/pnas.1607171113

Balch, J. K., Bradley, B. A., Abatzoglou, J. T., Nagy, R. C., Fusco, E. J., & Mahood, A. L. (2017). Human-started wildfires expand the fire niche across the United States. *Proceedings of the National Academy of Sciences*, *114*(11), 2946–2951. https://doi.org/10.1073/pnas.1617394114

Box, J. E., Colgan, W. T., Christensen, T. R., Schmidt, N. M., Lund, M., Parmentier, F.-J. W., et al. (2019). Key indicators of Arctic climate change: 1971–2017. *Environmental Research Letters*, *14*(4), 045010. https://doi.org/10.1088/1748-9326/aafc1b

Compo, G. P., Whitaker, J. S., Sardeshmukh, P. D., Matsui, N., Allan, R. J., Yin, X., et al. (2011). The Twentieth Century Reanalysis Project. *Quarterly Journal of the Royal Meteorological Society*, *137*(654), 1–28. https://doi.org/10.1002/qj.776

Dai, A. (2006). Recent Climatology, Variability, and Trends in Global Surface Humidity. *Journal of Climate*, *19*(15), 3589–3606. https://doi.org/10.1175/JCLI3816.1

Dai, A. (2011). Drought under global warming: a review. *Wiley Interdisciplinary Reviews: Climate Change*, *2*(1), 45–65. https://doi.org/10.1002/wcc.81

Dai, A., Trenberth, K. E., & Qian, T. (2004). A Global Dataset of Palmer Drought Severity Index for 1870–2002: Relationship with Soil Moisture and Effects of Surface Warming. *Journal of Hydrometeorology*, *5*(6), 1117–1130. https://doi.org/10.1175/JHM-386.1

Dee, D. P., Uppala, S. M., Simmons, A. J., Berrisford, P., Poli, P., Kobayashi, S., et al. (2011). The ERA-Interim reanalysis: configuration and performance of the data assimilation

system. *Quarterly Journal of the Royal Meteorological Society*, *137*(656), 553–597. https://doi.org/10.1002/qj.828

Dennison, P. E., Brewer, S. C., Arnold, J. D., & Moritz, M. A. (2014). Large wildfire trends in the western United States, 1984–2011. *Geophysical Research Letters*, *41*(8), 2928–2933. https://doi.org/10.1002/2014GL059576

Eidenshink, J. C., Schwind, B., Brewer, K., Zhu, Z.-L., Quayle, B., & Howard, S. M. (2007). A project for monitoring trends in burn severity. *Fire Ecology*, *3*(1), 321. https://doi.org/10.4996/fireecology.0301003

Feng, S., & Fu, Q. (2013). Expansion of global drylands under a warming climate. *Atmospheric Chemistry and Physics*, *13*(19), 10081–10094. https://doi.org/10.5194/acp-13-10081-2013

Free, M., Sun, B., & Yoo, H. L. (2016). Comparison between Total Cloud Cover in Four Reanalysis Products and Cloud Measured by Visual Observations at U.S. Weather Stations. *Journal of Climate*, *29*(6), 2015–2021. https://doi.org/10.1175/JCLI-D-15-0637.1

Fu, Q., Manabe, S., & Johanson, C. M. (2011). On the warming in the tropical upper troposphere: Models versus observations. *Geophysical Research Letters*, *38*(15). https://doi.org/10.1029/2011GL048101

Fu, R. (2015). Global warming-accelerated drying in the tropics. *Proceedings of the National Academy of Sciences*, *112*(12), 3593. https://doi.org/10.1073/pnas.1503231112

Gelaro, R., McCarty, W., Suárez, M. J., Todling, R., Molod, A., Takacs, L., et al. (2017). The Modern-Era Retrospective Analysis for Research and Applications, Version 2 (MERRA-2). *Journal of Climate*, *30*(14), 5419–5454. https://doi.org/10.1175/JCLI-D-16-0758.1

Guzman-Morales, J., & Gershunov, A. (2019). Climate Change Suppresses Santa Ana Winds of Southern California and Sharpens Their Seasonality. *Geophysical Research Letters*, *46*(5), 2772–2780. https://doi.org/10.1029/2018GL080261

Harvey, B. J. (2016). Human-caused climate change is now a key driver of forest fire activity in the western United States. *Proceedings of the National Academy of Sciences*, *113*(42), 11649–11650. https://doi.org/10.1073/pnas.1612926113

Holden, Z. A., Swanson, A., Luce, C. H., Jolly, W. M., Maneta, M., Oyler, J. W., et al. (2018). Decreasing fire season precipitation increased recent western US forest wildfire activity. *Proceedings of the National Academy of Sciences*, *115*(36), E8349–E8357. https://doi.org/10.1073/pnas.1802316115

Hu, Y., & Fu, Q. (2007). Observed poleward expansion of the Hadley circulation since 1979. *Atmospheric Chemistry and Physics*, *7*(19), 5229–5236. https://doi.org/10.5194/acp-7-5229-2007

Huang, J., Ji, M., Xie, Y., Wang, S., He, Y., & Ran, J. (2016). Global semi-arid climate change over last 60 years. *Climate Dynamics*, *46*(3), 1131–1150. https://doi.org/10.1007/s00382-015-2636-8

Hughes, M., Hall, A., & Kim, J. (2011). Human-induced changes in wind, temperature and relative humidity during Santa Ana events. *Climatic Change*, *109*(1), 119–132. https://doi.org/10.1007/s10584-011-0300-9

Jin, Y., Goulden, M. L., Faivre, N., Veraverbeke, S., Sun, F., Hall, A., et al. (2015). Identification of two distinct fire regimes in Southern California: implications for economic impact and future change. *Environmental Research Letters*, *10*(9), 094005. https://doi.org/10.1088/1748-9326/10/9/094005

Kanamitsu, M., Ebisuzaki, W., Woollen, J., Yang, S.-K., Hnilo, J. J., Fiorino, M., & Potter, G. L. (2002). NCEP–DOE AMIP-II Reanalysis (R-2). *Bulletin of the American Meteorological Society*, *83*(11), 1631–1644. https://doi.org/10.1175/BAMS-83-11-1631

Kasischke, E. S., & Turetsky, M. R. (2006). Recent changes in the fire regime across the North American boreal region—Spatial and temporal patterns of burning across Canada and Alaska. *Geophysical Research Letters*, *33*(9). https://doi.org/10.1029/2006GL025677

Kitzberger, T., Brown, P. M., Heyerdahl, E. K., Swetnam, T. W., & Veblen, T. T. (2007). Contingent Pacific–Atlantic Ocean influence on multicentury wildfire synchrony over western North America. *Proceedings of the National Academy of Sciences*, *104*(2), 543–548. https://doi.org/10.1073/pnas.0606078104

Kobayashi, S., Ota, Y., Harada, Y., Ebita, A., Moriya, M., Onoda, H., et al. (2015). The JRA-55 Reanalysis: General Specifications and Basic Characteristics. *Journal of the Meteorological Society of Japan. Ser. II*, *93*(1), 5–48. https://doi.org/10.2151/jmsj.2015-001

Lau, W. K. M., & Kim, K.-M. (2015). Robust Hadley Circulation changes and increasing global dryness due to CO_2 warming from CMIP5 model projections. *Proceedings of the National Academy of Sciences*, 201418682. https://doi.org/10.1073/pnas.1418682112

Lau, William Ka-Ming, & Kim, K.-M. (2017). Competing influences of greenhouse warming and aerosols on Asian summer monsoon circulation and rainfall. *Asia-Pacific Journal of Atmospheric Sciences*, *53*(2), 181–194. https://doi.org/10.1007/s13143-017-0033-4

Lau, William K.-M., Wu, H.-T., & Kim, K.-M. (2013). A canonical response of precipitation characteristics to global warming from CMIP5 models. *Geophysical Research Letters*, *40*(12), 3163–3169. https://doi.org/10.1002/grl.50420

Littell, J. S., McKenzie, D., Peterson, D. L., & Westerling, A. L. (2009). Climate and wildfire area burned in western U.S. ecoprovinces, 1916–2003. *Ecological Applications*, *19*(4), 1003–1021. https://doi.org/10.1890/07-1183.1

Littell, J. S., Peterson, D. L., Riley, K. L., Liu, Y., & Luce, C. H. (2016). A review of the relationships between drought and forest fire in the United States. *Global Change Biology*, *22*(7), 2353–2369. https://doi.org/10.1111/gcb.13275

Liu, Y., Stanturf, J., & Goodrick, S. (2010). Trends in global wildfire potential in a changing climate. *Forest Ecology and Management*, *259*(4), 685–697. https://doi.org/10.1016/j.foreco.2009.09.002

Liu, Y., Goodrick, S., & Heilman, W. (2014). Wildland fire emissions, carbon, and climate: Wildfire–climate interactions. *Forest Ecology and Management*, *317*, 80–96. https://doi.org/10.1016/j.foreco.2013.02.020

Lorenz, D. J., & DeWeaver, E. T. (2007). Tropopause height and zonal wind response to global warming in the IPCC scenario integrations. *Journal of Geophysical Research: Atmospheres*, *112*(D10). https://doi.org/10.1029/2006JD008087

Lu, J., Vecchi, G. A., & Reichler, T. (2007). Expansion of the Hadley cell under global warming. *Geophysical Research Letters*, *34*(6). https://doi.org/10.1029/2006GL028443

Miller, N. L., & Schlegel, N. J. (2006). Climate change projected fire weather sensitivity: California Santa Ana wind occurrence. *Geophysical Research Letters*, *33*(15). https://doi.org/10.1029/2006GL025808

Pan, X., Chin, M., Ichoku, C. M., & Field, R. D. (2018). Connecting Indonesian fires and drought with the type of El Niño and phase of the Indian Ocean dipole during 1979–2016. *Journal of Geophysical Research: Atmospheres*, 123(15), 7974-7988.

Picotte, J. J., Peterson, B. E., Meier, G., & Howard, S. M. (2016). 1984–2010 trends in fire burn severity and area for the conterminous US. *International Journal of Wildland Fire*, *25*(4), 413420. https://doi.org/10.1071/WF15039

Rossow, W. B., & Schiffer, R. A. (1991). ISCCP Cloud Data Products. *Bulletin of the American Meteorological Society*, *72*(1), 2–20. https://doi.org/10.1175/1520-0477(1991)072<0002:ICDP>2.0.CO;2

Running, S. W. (2006). CLIMATE CHANGE: Is Global Warming Causing More, Larger Wildfires? *Science*, *313*(5789), 927–928. https://doi.org/10.1126/science.1130370

Santer, B. D., Thorne, P. W., Haimberger, L., Taylor, K. E., Wigley, T. M. L., Lanzante, J. R., et al. (2008). Consistency of modelled and observed temperature trends in the tropical troposphere. *International Journal of Climatology*, *28*(13), 1703–1722. https://doi.org/10.1002/joc.1756

Santer, Benjamin D., Solomon, S., Pallotta, G., Mears, C., Po-Chedley, S., Fu, Q., et al. (2016). Comparing Tropospheric Warming in Climate Models and Satellite Data. *Journal of Climate*, *30*(1), 373–392. https://doi.org/10.1175/JCLI-D-16-0333.1

Schoennagel, T., Veblen, T. T., Romme, W. H., Sibold, J. S., & Cook, E. R. (2005). Enso and Pdo Variability Affect Drought-Induced Fire Occurrence in Rocky Mountain Subalpine Forests. *Ecological Applications*, *15*(6), 2000–2014. https://doi.org/10.1890/04-1579

Seager, R., & Vecchi, G. A. (2010). Greenhouse warming and the 21st century hydroclimate of southwestern North America. *Proceedings of the National Academy of Sciences*, *107*(50), 21277–21282. https://doi.org/10.1073/pnas.0910856107

Seager, R., Hooks, A., Williams, A. P., Cook, B., Nakamura, J., & Henderson, N. (2015). Climatology, variability, and trends in the US vapor pressure deficit, an important fire-

related meteorological quantity. *Journal of Applied Meteorology and Climatology*, 54(6), 1121-1141.

Seidel, D. J., & Randel, W. J. (2007). Recent widening of the tropical belt: Evidence from tropopause observations. *Journal of Geophysical Research: Atmospheres*, *112*(D20). https://doi.org/10.1029/2007JD008861

Seidel, D. J., Fu, Q., Randel, W. J., & Reichler, T. J. (2008). Widening of the tropical belt in a changing climate. *Nature Geoscience*, *1*(1), 21–24. https://doi.org/10.1038/ngeo.2007.38

Sherwood, S. C., Ingram, W., Tsushima, Y., Satoh, M., Roberts, M., Vidale, P. L., & O'Gorman, P. A. (2010). Relative humidity changes in a warmer climate. *Journal of Geophysical Research: Atmospheres*, *115*(D9). https://doi.org/10.1029/2009JD012585

Smith, A., Lott, N., & Vose, R. (2011). The Integrated Surface Database: Recent Developments and Partnerships. *Bulletin of the American Meteorological Society*, *92*(6), 704–708.

Sun, B., Free, M., Yoo, H. L., Foster, M. J., Heidinger, A., & Karlsson, K.-G. (2015). Variability and Trends in U.S. Cloud Cover: ISCCP, PATMOS-x, and CLARA-A1 Compared to Homogeneity-Adjusted Weather Observations. *Journal of Climate*, *28*(11), 4373–4389. https://doi.org/10.1175/JCLI-D-14-00805.1

Veblen, T. T., Kitzberger, T., & Donnegan, J. (2000). Climatic and Human Influences on Fire Regimes in Ponderosa Pine Forests in the Colorado Front Range. *Ecological Applications*, *10*(4), 1178–1195. https://doi.org/10.1890/1051-0761(2000)010[1178:CAHIOF]2.0.CO;2

Veraverbeke, S., Rogers, B. M., Goulden, M. L., Jandt, R. R., Miller, C. E., Wiggins, E. B., & Randerson, J. T. (2017a). Lightning as a major driver of recent large fire years in North American boreal forests. *Nature Climate Change*, *7*(7), 529. https://doi.org/10.1038/nclimate3329

Veraverbeke, S., Rogers, B. M., Goulden, M. L., Jandt, R. R., Miller, C. E., Wiggins, E. B., & Randerson, J. T. (2017b). Lightning as a major driver of recent large fire years in North American boreal forests. *Nature Climate Change*, *7*(7), 529–534. https://doi.org/10.1038/nclimate3329

Wang, S., Huang, J., He, Y., & Guan, Y. (2014). Combined effects of the Pacific Decadal Oscillation and El Niño-Southern Oscillation on global land dry-wet changes. *Scientific Reports*, *4*, 6651. https://doi.org/10.1038/srep06651

Westerling, A. L., Gershunov, A., Brown, T. J., Cayan, D. R., & Dettinger, M. D. (2003). Climate and Wildfire in the Western United States. *Bulletin of the American Meteorological Society*, *84*(5), 595–604. https://doi.org/10.1175/BAMS-84-5-595

Westerling, A. L., Hidalgo, H. G., Cayan, D. R., & Swetnam, T. W. (2006). Warming and Earlier Spring Increase Western U.S. Forest Wildfire Activity. *Science*, *313*(5789), 940–943. https://doi.org/10.1126/science.1128834

Wild, M. (2011). Enlightening Global Dimming and Brightening. *Bulletin of the American Meteorological Society*, *93*(1), 27–37. https://doi.org/10.1175/BAMS-D-11-00074.1

Willett, K. M., Dunn, R. J. H., Thorne, P. W., Bell, S., de Podesta, M., Parker, D. E., et al. (2014). HadISDH land surface multi-variable humidity and temperature record for climate monitoring. *Climate of the Past*, *10*(6), 1983–2006. https://doi.org/10.5194/cp-10-1983-2014

Williams, A. P., Seager, R., Berkelhammer, M., Macalady, A. K., Crimmins, M. A., Swetnam, T. W., et al. (2014). Causes and Implications of Extreme Atmospheric Moisture Demand during the Record-Breaking 2011 Wildfire Season in the Southwestern United States.

Journal of Applied Meteorology and Climatology, *53*(12), 2671–2684. https://doi.org/10.1175/JAMC-D-14-0053.1

Wuebbles, D. (2017). Climate Science Special Report: Fourth National Climate Assessment (NCA4), Volume I | GlobalChange.gov. Retrieved September 25, 2019, from https://www.globalchange.gov/browse/reports/climate-science-special-report-fourth-national-climate-assessment-nca4-volume-i

Yin, J. H. (2005). A consistent poleward shift of the storm tracks in simulations of 21st century climate. *Geophysical Research Letters*, *32*(18). https://doi.org/10.1029/2005GL023684

Yue, X., Mickley, L. J., & Logan, J. A. (2014). Projection of wildfire activity in southern California in the mid-twenty-first century. *Climate Dynamics*, *43*(7), 1973–1991. https://doi.org/10.1007/s00382-013-2022-3

Zeng, N., & Yoon, J. (2009). Expansion of the world's deserts due to vegetation-albedo feedback under global warming. *Geophysical Research Letters*, *36*(17). https://doi.org/10.1029/2009GL039699

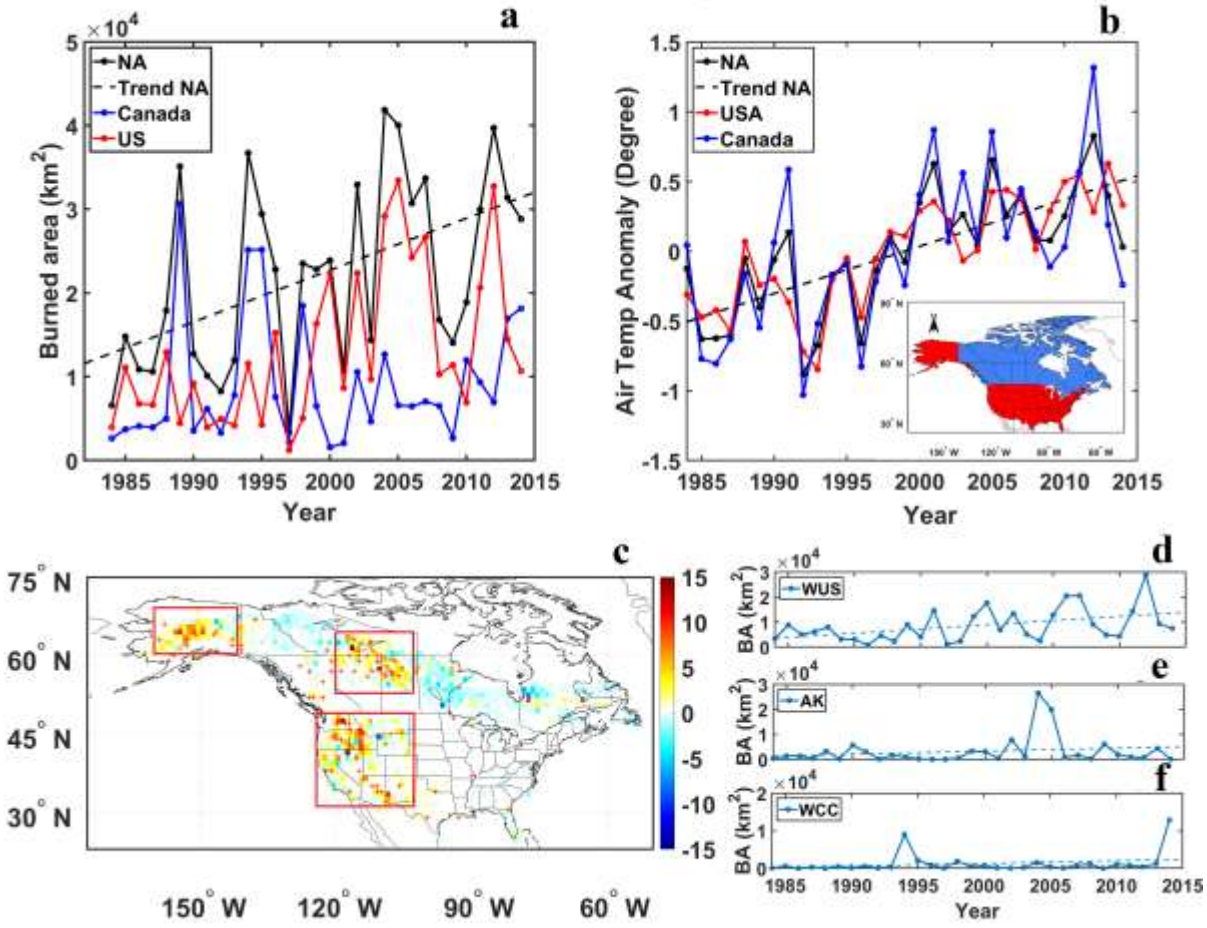

Fig.1 Wildfire trend over North America. Time series of a) burned area, and b) surface air temperature (^{o}C) over North America (black), US (red) and Canada (blue) respectively. Units of burned area in 10^4 km^2. Spatial pattern linear trend for c) burned area North America from 1984-2014 (May to September), unit in km^2 decade^{-1} per 1° by 1° grid size. Statistical significance ($p < 0.05$) are denoted by red cross. Lower right panels show time series of total burned area, and trend lines, averaged over domains marked by red rectangles, representing respectively d) Western US, e) Alaska, and f) Western Central Canada.

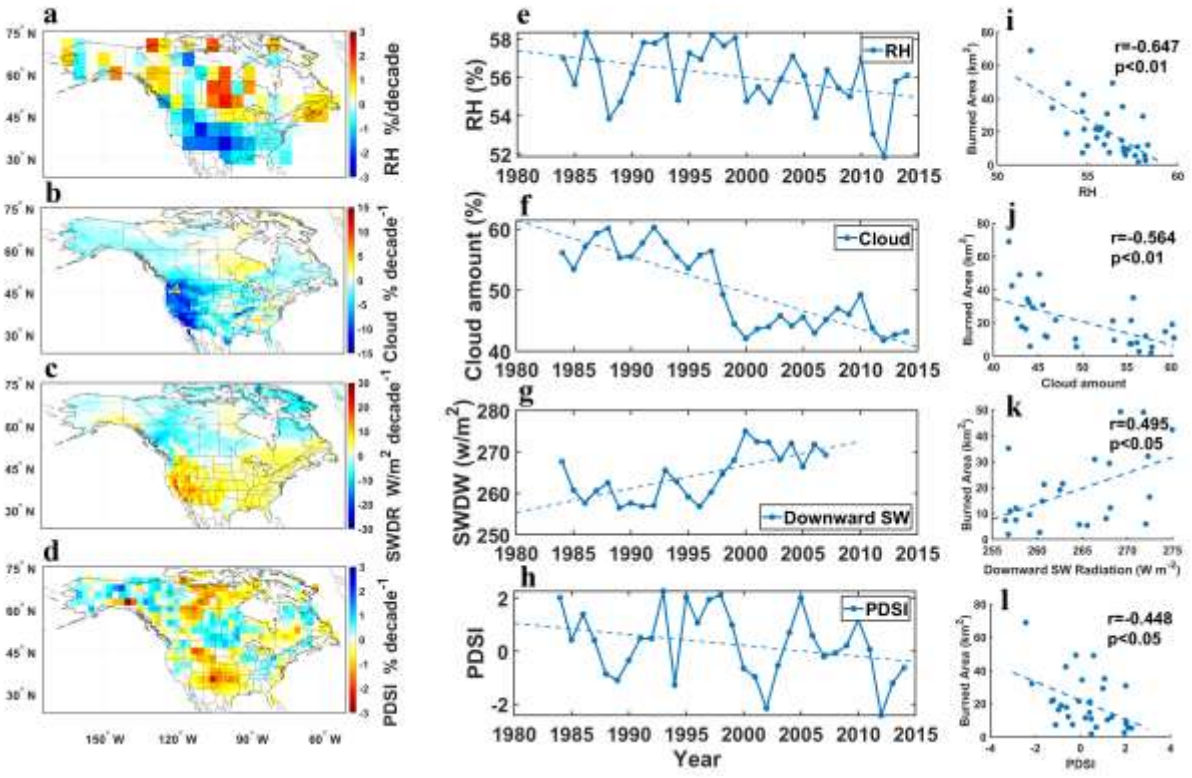

Fig.2 Temporal and spatial trend of observed climate variables. Spatial trend pattern of observed climate variables a) RH (% decade^{-1}), b) cloud (% decade^{-1}, c) downward SW radiation (wm^{-2} decade^{-1}), and d) PDSI over North America from 1984-2014. Time series of climate variables over Western US for e) RH, f) cloudiness, g) downward SW radiation and h) PDSI. Right panel (i, j, k, l) shows respectively, the scatter plot, and regression line of burned area vs. the corresponding variable.

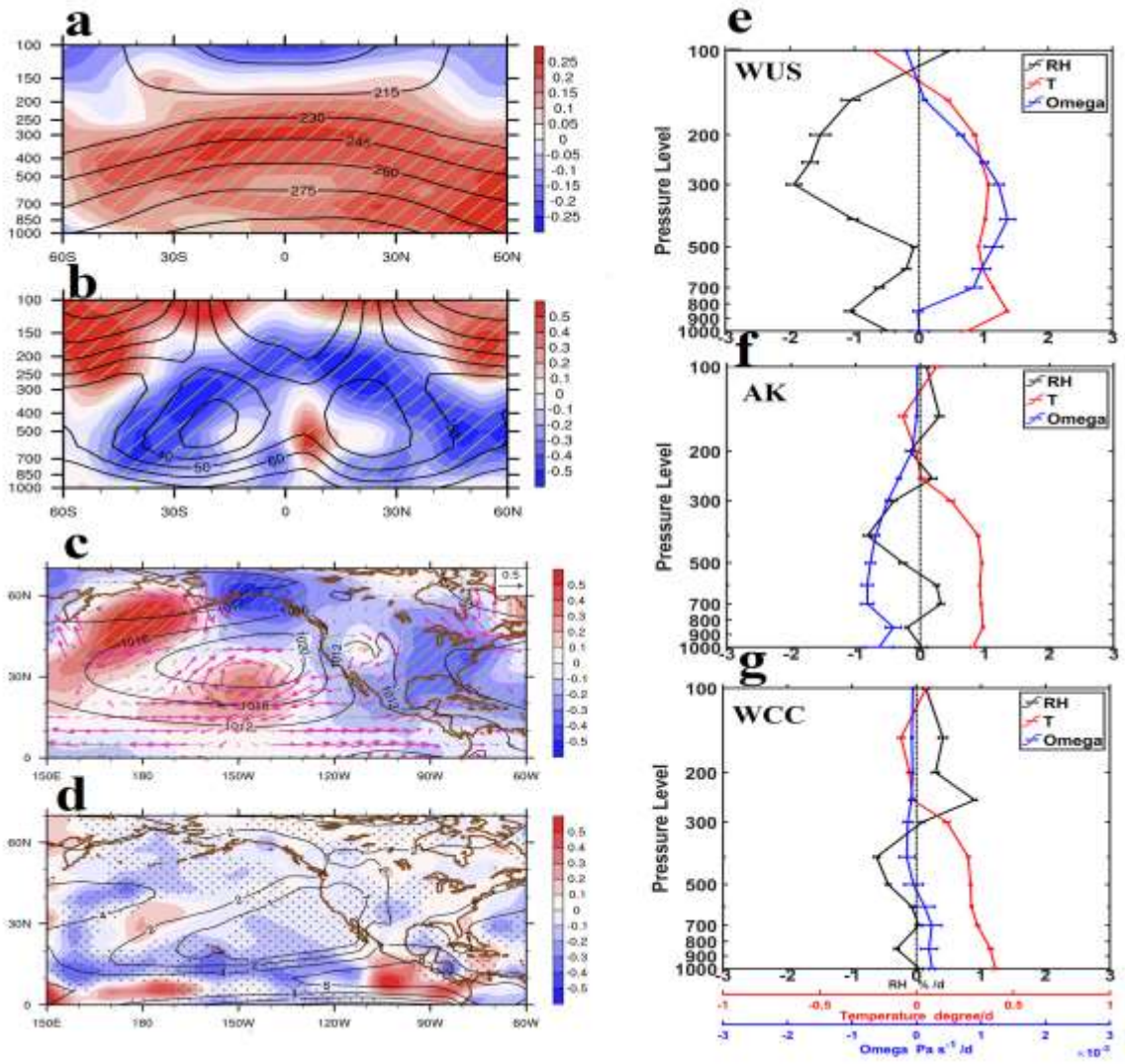

Fig.3 Latitude-height cross-section of zonal mean temperature trend in units of C° per decade (a) relative humidity trend in units of % per decade (b), Spatial pattern of trends of (c) sea level pressure (hPa decade^{-1}), and 700hPa winds (ms^{-1}decade^{-1}), and (d) precipitation (mm day^{-1}decade^{-1}) and vertical motion (Pa s^{-1} decade^{-1}). Anomalies are shown by color shading, and climatology by contours, and areas of anomalous descending motions are indicated by black dots. Vertical profiles of trends of temperature (shaded red, in ^{o}C decade^{-1}), RH (black line, in % decade^{-1}) and vertical p-velocity (blue line, in Pa s^{-1} decade^{-1}, with positive values denoting sinking motion for

(e) Western US, (f) Alaska and (g) Western Central Canada, based on the ensemble mean of five reanalysis data. Standard errors of the mean are shown as horizontal error bars.